Crevice Corrosion Study of Materials for Propulsion Applications in the Marine Environment

F. Deflorian[1,†], S. Rossi[1], M. Fedel[1], C. Zanella[1,2], D. Ambrosi[1], and E. Hlede[3]

[1]*Department of Industrial Engineering, University of Trento, via Sommarive 9, Trento, Italy*
[2]*SP Technical Research Institute of Sweden, Jönköping University, Jönköping, Sweden*
[3]*Wärtsilä Italy S.p.A., Bagnoli della Rosandra 334, San Dorligo della Valle, Trieste*
(Received July 22, 2015; Revised December 02, 2015; Accepted December 02, 2015)

The present work addresses crevice and galvanic corrosion processes occurring at the cylinder head gasket/cylinder head interface and cylinder head gasket/cylinder liner interface of four-stroke medium-speed diesel engines for marine applications. The contact between these systems and the marine environment can promote formation of demanding corrosion conditions, therefore influencing the lifetime of the engine components. The electrochemical behavior of various metals and alloys used as head gasket materials (both ferrous alloys and copper alloys) was investigated. The efficacy of corrosion inhibitors was determined by comparing electrochemical behavior with and without inhibitors. In particular, crevice corrosion has been investigated by electrochemical tests using an experimental set-up developed starting from the requirements of the ASTM G-192-08, with adaptation of the test to the conditions peculiar to this application. In addition to the crevice corrosion resistance, the possible problems of galvanic coupling, as well as corrosive reactivity, were evaluated using electrochemical tests, such as potentiodynamic measurements. It was possible to quantify, in several cases, the corrosion resistance of the various coupled materials, and in particular the resistance to crevice corrosion, providing a basis for the selection of materials for this specific application.

Keywords : *head gasket, crevice corrosion, galvanic corrosion*

1. Introduction

Medium speed four-stroke diesel engines are commonly used to power marine propulsion systems. Similar to the engines equipping ground vehicles, "medium-speed engines" consists in a cylinder liner-connected to the cylinder head by means of an head gasket interposed between the two components. The presence head gasket prevents the release of pressure gasses from the combustion chamber, thus improving the engine efficiency, and accommodates the thermal expansion of the cylinders head and cylinder liner due to the heat generated during fuel combustion. Moreover, the gasket material is subjected to wear and fretting due to the relative sliding of the different component during thermal expansion and/or shrinkage. Owing to the heat generated during combustion, the engine components, as well as the head gasket, are cooled using a water based refrigerant. Fig. 1 depicts a schematic representation of a common strategy to control the engine temperature by cooling, at the same time, cylinders head,

head gasket and cylinder liner. Observe that the gasket is affected by the combustion by-products, heat and pressurized gas on the inner side, while the outer side is directly in contact with the cooling fluid. In addition, notice that the cooling circuit is closed and is therefore expected not to be rich in oxygen.

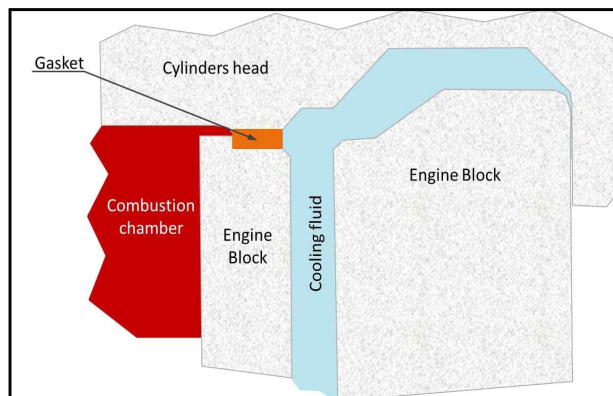The presence of a water based cooling fluid can promote severe problems of corrosion, influencing therefore

Fig. 1. Schematic representation of the Cylinder liner / engine block / cylinder gasket head / cylinders head system.

---

† Corresponding author: flavio.deflorian@unitn.it

the engine durability and reliability. The corrosion process, not only promoted by the aggressiveness due to the possible presence of chlorides, is also enhanced by the activation of galvanic coupling phenomena[1] among the different metal component in the engine. The present work deals with the study of crevice corrosion processes[2,3] occurring at the head gasket/cylinders head interface and head gasket/ cylinder liner interface of propulsion systems for marine applications. The phenomenon is expected to be influenced by the galvanic coupling between the material of the gasket and the cylinder liner/cylinder head, since they are different due to specific mechanical properties requirements. Crevice and galvanic coupling phenomena were studied in a laboratory scale with specific experimental set-up adapted to simulate harsh crevice conditions as well as the effect of a galvanic action. For this purposes, different metals were investigated in terms of crevice corrosion resistance and electrochemical behaviour while forming a galvanic couple. In particular, copper alloys, austenitic stainless steels and mild steel were tested. These alloys were chosen among the most common head gasket materials because of their suitable mechanical and wear resistance for the specific application. Real portion of effective gaskets were exploited. In addition, also the cylinder liner and cylinder head materials were tested: grey cast iron and ductile cast iron samples were subjected to the electrochemical analysis. Polarization curves have been performed in order to characterize the materials under investigation. The electrochemical characterization of the different metals was carried out at 80 °C (temperature reached by the cooling fluid during normal operation) in both in a neutral electrolyte as well as in an electrolyte containing a corrosion inhibitor. Crevice corrosion tests were carried out following the guidelines of ASTM G-192-08 standard: the crevice re-passivation potential has been determined and used to compare the crevice corrosion susceptibility of the different metals. All the electrochemical measurements were carried out both in aerated as well as in de-aerated (by means of nitrogen bubbling) solutions. The effect of the galvanic action at the gasket/cylinder head and gasket/ cylinder liner interface (see Fig. 1) was investigated by monitoring potential and current flow evolution during about 20 of galvanic coupling in the electrolyte.

2. Experimental Procedure

The metallic samples were cut from effective head gaskets for medium-speed engines made of aluminium bronze, nickel bronze, austenitic stainless steel without Mo, austenitic stainless steel with Mo and mild steel (Table 1).

50 x 20 x 5 mm lamellar and spheroidal cast iron samples were cut from real engine components using a CNC cutter. Fig. 2 shows an example of the appearance of the samples.

The electrolyte used to carry out the electrochemical measurements consisted in 80 g/l NaCl + 150 g/l Na_2SO_4 water based solution. Measurements were carried out also in presence of a corrosion inhibitor. The corrosion inhibitor employed was added to the electrolyte at a 5 % v/v concentration. It contains benzotriazole compounds. The pH of the neat electrolyte was 5,3 (at 25 °C); when the corrosion inhibitor is added to the solution, the pH raises to 10.3 (at 25 °C). For the polarization curves a three-electrode arrangement was used: the working electrode was the investigated sample while platinum rings were employed as counter and reference electrodes. The potential sweep ranged from -0.030 V vs OCP to the voltage corresponding to a current density value of 10^{-4} A/cm², assumed as a threshold value beyond which the corrosion rate becomes noticeably high. The scan rate was set to 0,167 mV/s. The immersed area was about 12 cm². The crevice corrosion resistance was evaluated following the guidelines of the "Tsujikawa-Hisamatsu Electrochemical

Table 1. Samples under investigation

Metal/alloy	Label
Copper – Aluminium alloy	Cu-Al
Copper – Nickel alloy	Cu-Ni
Austenitic stainless steel without Mo	S.S.
Austenitic stainless steel with Mo	S.S.-Mo
Mild steel	Mild steel

Fig. 2. Appearance of the metal samples: austenitic stainless steel without Mo (1), Nickel bronze (2) and lamellar cast iron (3).
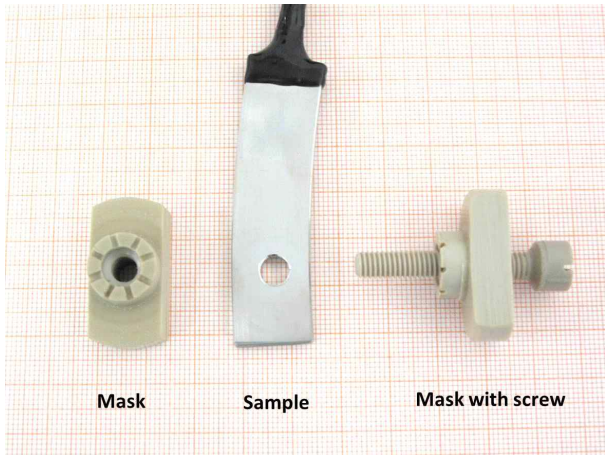
Fig. 3. Two-part PEEK mask.

Fig. 4. Experimental set-up: the arrow indicates the PEEK mask exploited to promote crevice corrosion.

(THE) test method" [4]. The test was carried out exploiting the experimental set-up proposed in ASTM G192–08 standard, which was successfully exploited by other authors[5,6]. A PEEK mask (Fig. 3) was used to produce the geometrical conditions to promote the occurrence of crevice corrosion. The two-part mask consists of two PEEK circular crown with small gorges which are forced against the metal sample by means of a screw (Fig.ure 4). The two parts are connected by means of the screw which is loaded with a 0,20 N/m torque.

The "Tsujikawa-Hisamatsu Electrochemical (THE) test method" consist of a multi-step electrochemical test:

1. Polarization measurement starting 100 mV below OCP and progressing anodically (0,0167 mV/s) until a pre-specified current density is reached;
2. Galvanostatic conditioning at the end current in the previous step for 2 h (to grow the crevice corroded area) monitoring the potential output;
3. Potentiostatic conditioning at the end potential in the previous step minus 10 mV for 2 h monitoring the current density output;
4. If the current increases with time during the step 3. another potentiostatic period of 2 h was applied subtracting another 10 mV to the previously applied potential: decreasing steps of 10 mV were repeated until the output current density decreased with time in the 2 h period;

Fig. 5 depicts the example reported in[4] to explain the "THE" method: potential and current density are collected/imposed during the different steps of the electrochemical test method.

All the electrochemical tests were carried out at 80 °C both in aerated and de-aerated conditions. De-aeration was obtained by means of N_2 bubbling in the solution: the
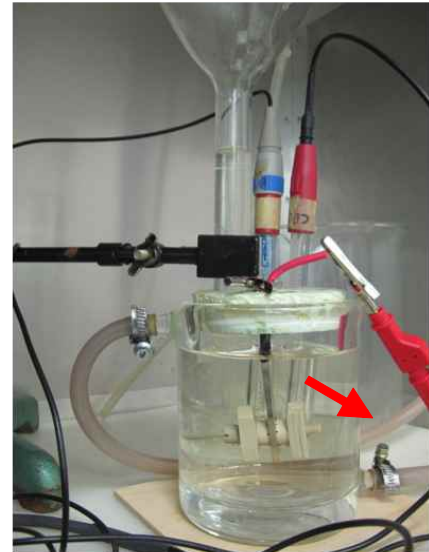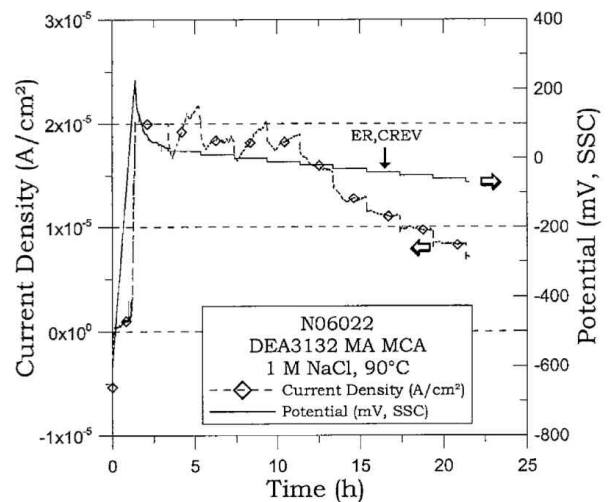

Fig. 5. Example of "Tsujikawa-Hisamatsu Electrochemical (THE) test method", from[4].

oxygen content decreased from 4,1 ppm to less than 1 ppm. A Metrohm Autolab PGSTAT302N Potentiostat was employed. A Faraday cage was used to minimize external interference on the system. Eventually, galvanic coupling current was measured between the head gasket materials (Aluminium bronze, Nickel bronze, two austenitic stainless steels grades, and mild steel) and the cylinder head metal (ductile cast iron). The electrodes were immersed in the electrolyte containing the corrosion inhibitor at 80 °C under nitrogen bubbling. The extent of the immersed area was maintained constant for each sample. A PAR Parstat 2273 was employed to measure the current flowing
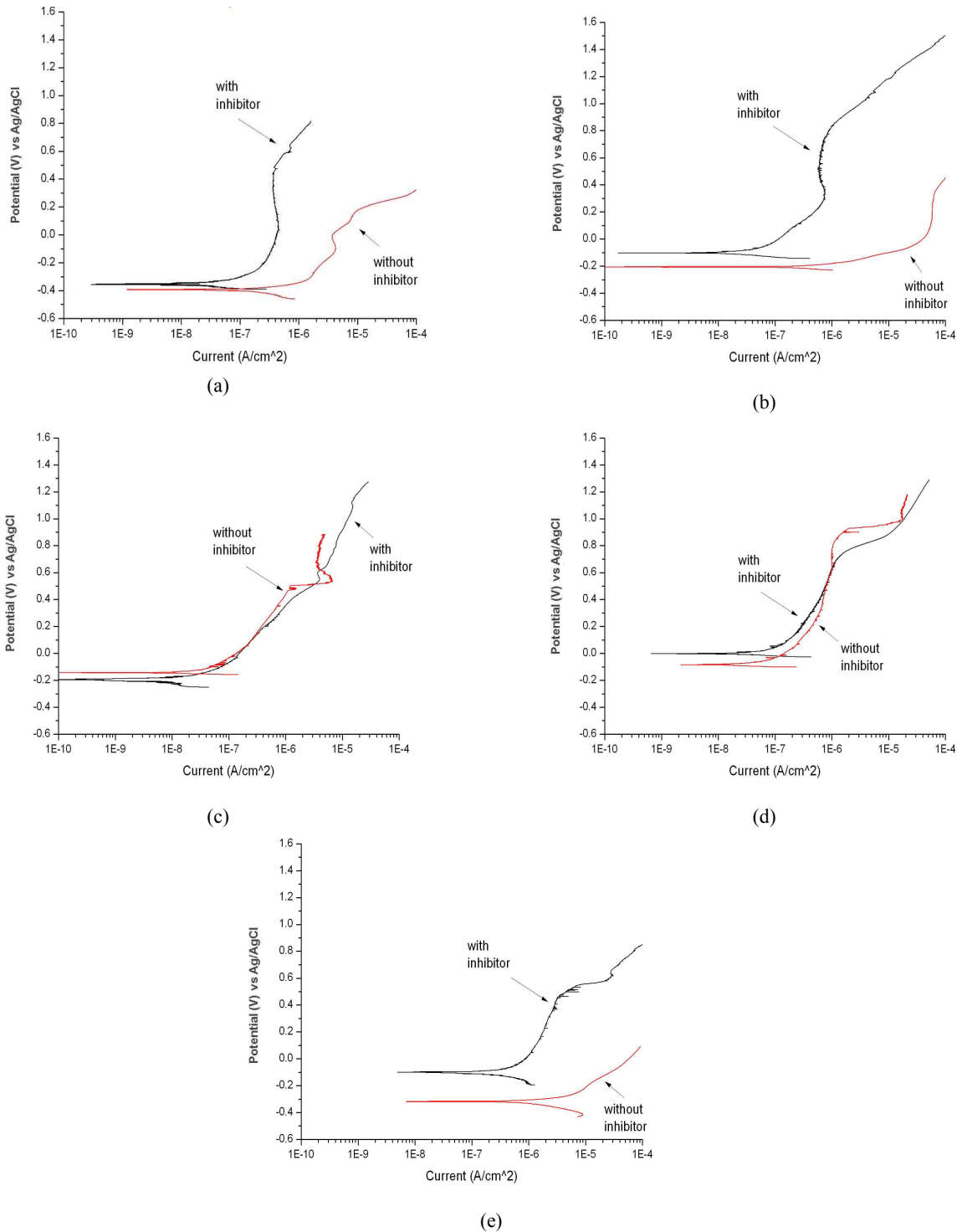
Fig. 6. Polarization curves: (a) Aluminium bronze, (b) Nickel Bronze, (c) S.S., (d) S.S.-Mo and (e) mild steel.

between the electrodes.

3. Results and Discussion

3.1 Polarization curves

Polarization curves were carried out in order to evaluate the effect of the electrolyte and the influence of the corro-

F. DEFLORIAN, S. ROSSI, M. FEDEL, C. ZANELLA, D. AMBROSI, AND E. HLEDE

sion inhibitor on the different metals. Fig. 6 (a-d) shows the experimental results for the head gaskets materials. From Fig. 6 it is possible to observe that the corrosion inhibitor seems efficient in decreasing anodic corrosion current for the Cu-Al alloy, Cu-Ni alloy and mild steel samples. The presence of the corrosion inhibitor shifts the anodic currents of the Cu-Al, Cu-Ni and mild steel samples to lower values, around 10^{-6} A/cm^2. On the other hand, stainless steel substrates are not influenced by the presence of the corrosion inhibitor. However, it should be noted that the anodic currents measured on S.S. and S.S.-Mo samples are relatively low ($10^{-6} \div 10^{-7}$ A/cm^2) and, therefore, the corrosion inhibitor is not able to further reduce the corrosion rate. Since the cooling fluid is in contact with engine component (different from the head gasket) such as cylinder liner and cylinder head, the effect of the electrolyte with and without the corrosion inhibitor was tested also on grey cast iron and ductile cast iron samples. Fig. 7 shows the polarization curves for the cast iron samples.

Considering Fig. 7, one can notice that the inhibitor promotes a certain reduction of the anodic current on both samples. However the beneficial effect (in terms of current reduction) is not as remarkable as for Cu-Al, Cu-Ni and mild steel samples.

Considering that the present work deals with the comparison of different metals, characterized by different electrochemical properties, in order to perform a consistent comparison, 100 times the steady state current density measured by means of polarization curves was selected as the threshold value of the current density to be employed in step 1. and 2. of the "THE" test. The reason

of this selection resides in trying to force crevice corrosion to occur on different metals in the most comparable way.

3.2 Crevice repassivation potential determination

Crevice repassivation potential determination test was carried out on the different metals both in aerated and de-aerated conditions. All the "THE" tests were carried out in the electrolyte containing 5v/v% of corrosion inhibitor. Fig. 8 depicts the appearance of a metal sample after the crevice repassivation potential determination test (in particular, the Cu-Al sample is reported). Notice that a crevice corrosion process took place in correspondence of the area which was partially covered by the PEEK mask in order to promote the formation of differential aeration cells.

As an example, Fig. 9 (a,b) shows the crevice repassivation potential determination for mild steel (a) and S.S.-Mo (b) samples in de-aerated conditions. For mild steel in de-aerated conditions (Fig. 9a) it was possible to determine a crevice corrosion repassivation potential at -0.349 V, obtained after six decreasing step (10 mV each) of the potential conditioning. Considering S.S.-Mo sample (Fig. 9b), repassivation occurred immediately after the switch off of the galvanostatic conditioning at the constant current density. This behaviour is clearly related to a very high crevice corrosion resistance of S.S.-Mo substrate under the conditions considered in the present study.

Considering the "THE" tests carried out in de-aerated solution on the different samples, the stainless steels, Cu-Al and Cu-Ni, showed a crevice repassivation potential immediately after the switch off of the galvanos-tatic superimposition of the constant current density. On the other hand, mild steel and cast irons samples requested a multiple 10
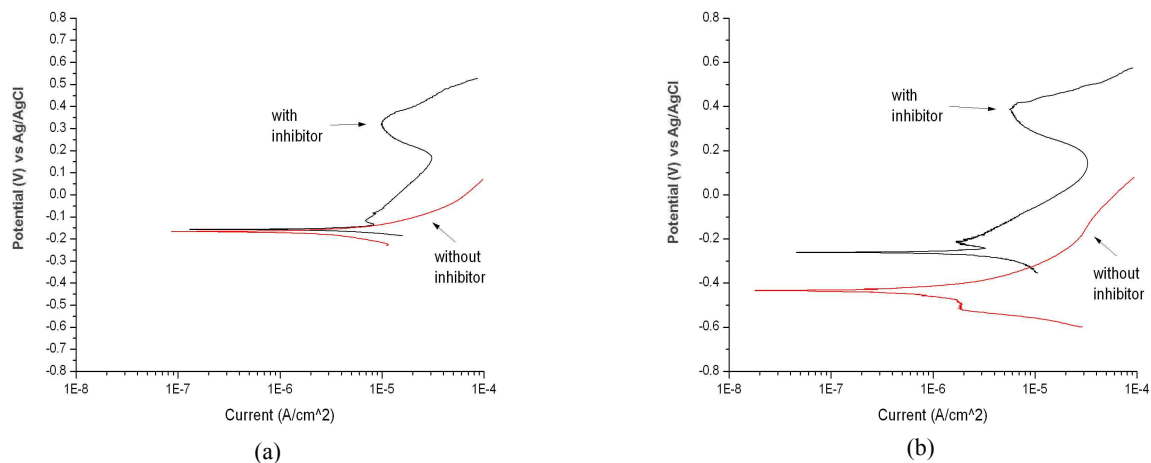

(a)

(b)

Fig. 7. Polarization curves for the engine components materials: (a) grey cast iron and (b) Ductile cast iron.
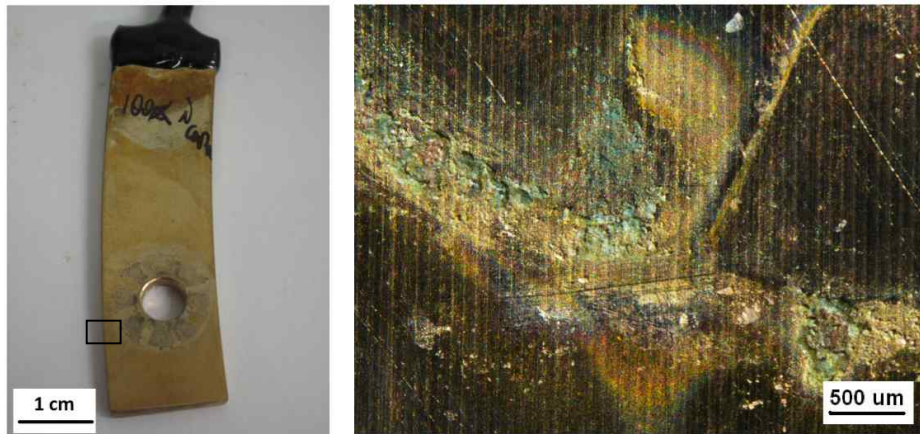
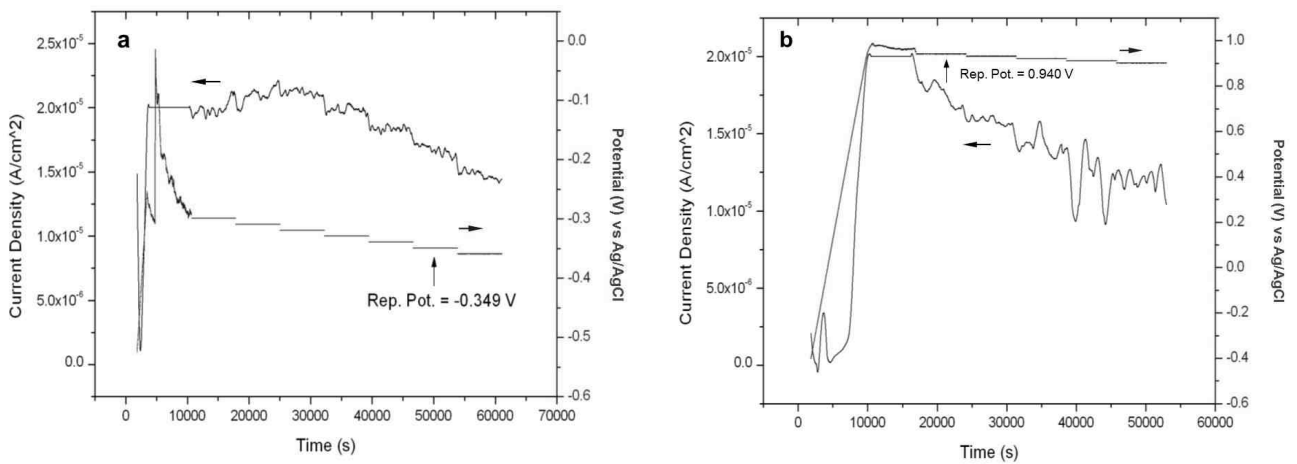**Fig. 8.** Appearance of the Cu-Al samples after "THE" crevice corrosion test.

Fig. 9. Crevice corrosion repassivation potential and corresponding currents for (a) mild steel sample and for (b) S.S.-Mo sample.
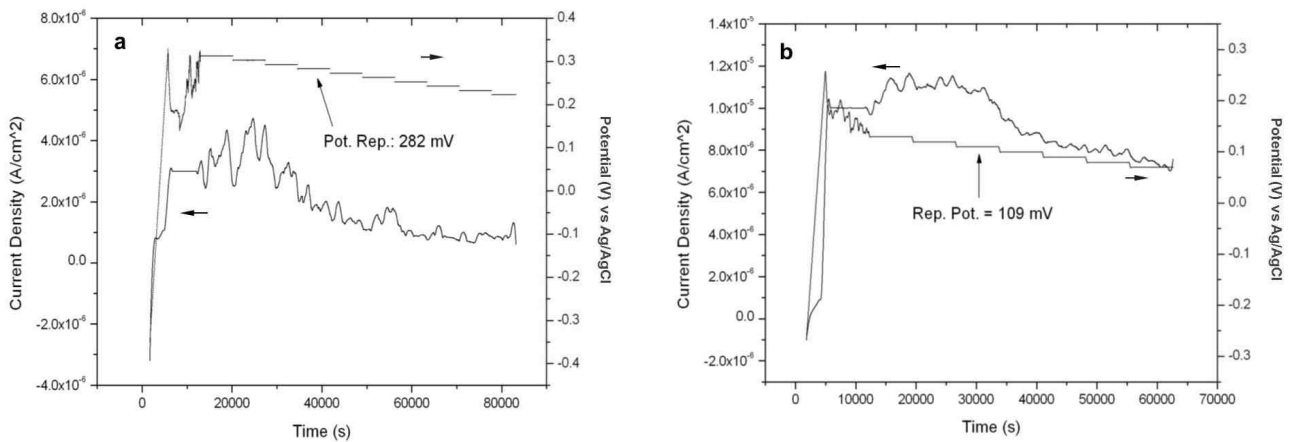

Fig. 10. Crevice corrosion repassivation potential and corresponding currents for (a) Cu-Ni and for (b) Cu-Al.

mV decreasing steps before reaching the crevice corrosion repassivation potential.

The "THE" test to determine the crevice repassivation potential was performed also in aerated conditions. Increasing the oxygen content in the electrolyte from less than 1 ppm (de-aerated conditions) to about 4,1 ppm

(aerated conditions), it is possible to observe that differently from the previous case, Cu-Ni and Cu-Al samples need a certain number of 10 mV decreasing steps to reach a crevice corrosion repassivation potential after the galvanostatic conditioning (Fig. 10). In fact, in aerated conditions, only stainless steels samples are able to repassivate immediately after the switch off of the galvanostatic current superimposition.

The crevice corrosion repassivation potentials for the samples under investigation are reported in Table 2. As previously anticipated, the stainless steels samples show an almost immediate repassivation after the end of the galvanostatic conditioning both in aerated and de-aerated conditions. The presence of higher oxygen content seems to promote the formation of a harsher environment, probably due to the more significant oxygen gradient which is formed in correspondence of the artificial crevice. In particular, compared to the behaviour in the de-aerated solution, samples Cu-Ni and Cu-Al do not show crevice repassivation potential immediately after the end of the galvanostatic conditioning and a certain number of 10 mV decreasing steps is required to repassivate.

3.3 Galvanic coupling

Galvanic coupling current was measured between Cu-Al, Cu-Ni, S.S.-Mo, S.S. and mild steel samples coupled with ductile cast iron, thus simulating the real operating conditions, where engine components and head gaskets are in contact. Table 3 shows the steady state current measured after about 20 h of coupling in the electrolyte containing the corrosion inhibitor.

Considering the galvanic coupling currents, first of all it is worth to notice that the positive values in Table 2 indicates that the anode of the galvanic couple correspond to the ductile cast iron electrode. Therefore, it seems that in the corrosion inhibitor containing electrolyte the gasket material are cathodically protected by the cast iron of the engine components. In addition, the experimental data reported in Table 2 indicates that the lower currents are related to the Cu-Ni / ductile cast iron couple which seems the less active. Stainless steels coupled with cast iron shows intermediate values of the current flowing between the metals, while the highest currents are observed for Cu-Al / ductile cast iron and Mild steel / ductile cast iron couples. Comparing the two copper alloys, relatively low corrosion current of the Cu-Ni / ductile cast iron couple compared to Cu-Al / ductile cast iron is likely to be related to the presence of Ni in the alloy. Considering that the crevice corrosion takes place at the interface of two different metals, the driving force for the galvanic corrosion is expected to play an important role for the initiation and propagation of the localized phenomena.

4. Conclusions

In this paper different metals were investigated as potential candidates as head gaskets materials. In particular, an aluminium bronze, a nickel bronze, two austenitic stainless steels grades and mild steel samples were investigated due to their suitable mechanical and wear resistance for the specific application object of the study. the stainless steels samples proved to be the most efficient

Table 2. Crevice repassivation potential of the investigated samples; the symbol [*] indicates that repassivation occurred immediately after galvanostatic conditioning

Sample	Crevice repassivation potential (mV)	
	De-aerated conditions ($O_2 <$ 1 ppm)	Aerated conditions ($O_2 \approx 4,1$ ppm)
S.S.-Mo	[*]	[*]
S.S.	[*]	[*]
Cu-Ni	[*]	282
Cu-Al	[*]	109
Ductile cast iron	275	92
Mild steel	-349	-361

Table 3. Galvanic coupling current after 20 h of immersion in the electrolyte containing the inhibitor

Galvanic couple	Galvanic coupling current ($\mu A/cm^2$)
S.S.-Mo / ductile cast iron	2,62
S.S. / ductile cast iron	2,34
Cu-Ni / ductile cast iron	1,33
Cu-Al / ductile cast iron	3,91
Mild steel / ductile cast iron	3,17

metals, among the studied ones, in terms of corrosion resistance as well as the less susceptible to crevice corrosion, both in aerated and de-aerated conditions. However, relatively high corrosion currents were measured when stainless steels samples are coupled with the engine components metal (cast iron) thus indicating a certain tendency to promote corrosion of the cast iron at the interface between the two metals. Cu-Ni sample showed a relatively good crevice corrosion resistance (actually very high in de-aerated conditions), good corrosion resistance in presence of the inhibitor (anodic current in the 10^{-6} A/cm^2 range) and the galvanic coupling current were the lowest among the studied materials. In this sense, the austenitic stainless steels and the Cu-Ni alloy seems to be suitable materials to be used as cylinder head gaskets for four stroke medium speed engines. Among them, stainless steels seem slightly more effective, in particular concerning the crevice corrosion resistance. The other alloys, Cu-Al and mild steel, showed relatively good corrosion resistance in presence of the corrosion inhibitor and, at least for Cu-Al alloy, a relatively good crevice corrosion resistance. However, both samples showed the highest galvanic coupling currents, thus suggesting that the tested composition cannot be considered suitable for the specific application object of the present study.

References

1. L. J. Korb, D. L. Olson (Ed.s), ASM Handbook, Volume 13 - Corrosion, 4th ed., p. 183, ASM International, Ohio, USA (1992).
2. L. L. Shreir, R. A. Jarman, G. T. Burstein, Corrosion Volume 1, Metal/Environment reaction, 3rd ed., p. 1:151, Butterworth-Heinemann, Oxford, UK (2000).
3. R. Winston Revie (Ed.), Uhlig's Corrosion Handbook, 2nd ed., p. 173, John Wiley, Toronto, Canada (2000).
4. ASTM G192–08, Tsujikawa--Hisamatsu Electrochemical (THE) test method, ASTM International, West Conshohocken, PA (2014).
5. X. He, D. S. Dunn, A. A. Csontos, *Electrochim. Acta*, **52**, 7556 (2007).
6. N. S. Zadorozne, C. M. Giordano, M. A. Rodríguez, R. M. Carranza, R. B. Rebak, *Electrochim. Acta*, **76**, 94 (2012).